Extending the Fitzhugh Nagumo Excitable Tissue Model to Myocardial Necrosis

Aaron R. Shifman, Christopher B. Cole[1]

University of Ottawa

[1]BIO4134 Final Project

"In general, throughout the work, what is new is not good; and what is good is not new" - ***Reverend Martin Sherlock****, 1781*

Abstract

Neuroscience frequently relies on robust mathematical models to simulate and investigate trends in neuromechanics and signal propagation. We propose an examination of the Fitzhugh-Nagumo model, and additionally propose a modified extension of this model to account for necrosis of cardiac cells. We use this model to investigate case studies in myocardiac necrosis and examine the effect of necrosis on a one dimensional cardiac model.

Contents

List of Figures

Chapter 1

The Fitzhugh-Nagumo Model

The modelling of neurons and associated action potentials started in the early 1900s with the "integrate and fire" model.[1] In 1952, Hodgkin and Huxley created a biologically relevant 4 dimensional system of equations to describe neuron dynamics at a point.[2] While very interesting to biologists, mathematicians found the model too difficult to systematically study. In 1961 Richard Fitzhugh created a 2D caricature of the Hodgkin Huxley model (activation and recovery) using a modified Van der Pol oscillator.[3] This model has been both well studied and well characterized. Additionally, it has found many uses in cardiac models due to its simplicity and similarity in shape to a cardiac action potential.

The Hodgkin Huxley equations described how neuronal membrane voltage changed over time, given a large number of parameters.

$$\begin{aligned} C_m \frac{dV}{dt} &= I_m = I_{Na} + I_K + I_l \\ I_x &= \bar{G_x} p_{open}(V_m - E_x); x \in \{Na, K, l\} \\ p_{open_K} &= n^4 \\ p_{open_{Na}} &= m^3 h \\ p_{open_l} &\equiv 1 \\ \frac{dx}{dt} &= \alpha_x(V)(1-x) - \beta_x(V)x; x \in \{m, n, h\} \end{aligned}$$

This model is impossible to solve analytically, and quite difficult to explore numerically due to both the high dimensionality of the system and the

large number of parameters. In studying hyperplanes through the 4D phase space, Nagumo noticed that all planes of activation and recovery variables had a similar shape, so he tried modeling neuronal activity as a modified Van der Pol oscillator (Bonheffer-Van der Pol oscillator). This model, while not looking like stereotyped action potentials, has several features of the full hodgkin huxley model such as activation hysteresis and spike blocking. Despite not looking like a neuronal action potential, it closely resembles cardiac action potentials and have since been adapted as one of the de-facto models for cardiac simulations.

1.1 Model Rationale and Variables

The system presents in the following, non-dimensionalized form. This is not the original Bonheffer-Van der Pol model, however it is topologically equivalent and much easier to analyse. All models which follow are non-dimensionalized.

$$\frac{dV}{dt} = V(\alpha + V)(1 - V) - W + z$$
$$\frac{dW}{dt} = \beta V - cW$$

In this model V - in general - represents activation, and in an excitable tissue context represents voltage. W - in general - represents recovery, and has no realistic interpretation in a biological context, it would be the sum of all positive (with respect to the cell) currents. There are four parameters in the model, α, β, c, and z. Of the four parameters, we have significant interest in z, as it will determine the bifurcation of the model. Experimentally, z represents the DC (direct current) offset from experimentally injected current of the neuron under study. The additional parameters α, β, and c represent "rate - like" constants which determine oscillator traits such as amplitude, frequency, duty cycle, and excitability.

1.2 Purpose of Model and Examination

This model, a simplification of the original Hodgkin Huxley model, intends to model spiking cardiac myocytes. Tuning the individual parameters can adapt the model to fit various states and conditions which may be investigated by researchers. These models can be put together to form networks of neurons. The state of the neuron relies on the z parameter. In this project,

we plan to evaluate the stability of system at rest and with regards to the bifurcation parameter z. We plan to evaluate how the system responds and bifurcates with regards to this parameter, and interpret these stabilities biologically.

Figure 1.1: Time series of V and W following the Fitzhugh Nagumo model. $\alpha = 0.01, \beta = 0.5, c = 0.1, z = 0.5$

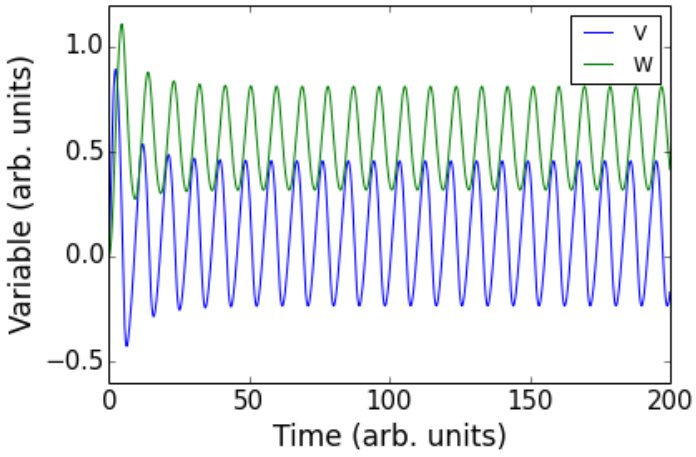

Initially, we present a naive time series of the model. We notice that with the set of parameters presented in Izhikevich 2006, the system oscillates in a stable limit cycle.[4] These parameters, utilized throughout the rest of this report unless otherwise noted, are as follows:

$$\alpha = 0.01$$
$$\beta = 0.5$$
$$c = 0.1$$
$$z = 0.5$$

Using the above parameters, we plot the system on the interval $t \in [0, 200]$ with arbitrary units for time in **Figure 1.1**. Note that the system is solved through an adaptive solver **odeint** in Python 2.

1.3 Model Classification

We classify the system according to the criterion established by Haefner et. al [3] and find the model is:

1. **Mechanistic** rather than phenomenological. Fitzhugh Nagumo (FN) models neural dyanmics as a function of individual processes acting on the neuron, including terms analagous to the DC offset, excitation, and relaxation. In this way, the model details the process of neural excitation and is process oriented.

2. **Dynamic** rather than static. The system models excitation and relaxation as a function of time, and is thus a dynamic model.

3. **Continuous** rather than discrete. The model uses time on an arbitrary scale as a continuous variable, instead of taking predefined "steps". In this way, the system uses time continuously.

4. **Spatially homogenous** rather than spatially heterogeneous. The model contains no explicit description of space, and is thus homogeneous.

5. **Deterministic** rather than stochastic. All terms in the model are entirely determined given initial conditions and no events based on chance occur. Thus the model is deterministic.

1.4 Stability Analysis

Taking the model such that:

$$f(x) = \dot{V} = V(\alpha + V)(1 - V) - W + z$$
$$g(x) = \dot{W} = \beta V - cW$$

We compute the Jacobian Matrix $\vec{J}$:

$$\vec{J} = \begin{bmatrix} \frac{\partial f}{\partial V} & \frac{\partial f}{\partial W} \\ \frac{\partial g}{\partial V} & \frac{\partial g}{\partial W} \end{bmatrix} = \begin{bmatrix} 2\alpha V + \alpha + (2 - 3V)V & -1 \\ \beta & -c \end{bmatrix}$$

Taking α, β, c equal to 0.01, 0.5, 0.1 respectively,

$$\begin{bmatrix} 0.02V + (2 - 3V)V + 0.01 & -1 \\ 0.5 & -0.1 \end{bmatrix}$$

Eigenvalues 1 and 2 are as follows

$$\lambda_{1,2} \approx \frac{1}{2} \begin{bmatrix} -3V^2 - 1.98V + \sqrt{9V^4 + 11.88V^3 + 3.2604V^2 - 0.4356V - 1.9879} - 0.09 \\ -3V^2 - 1.98V - \sqrt{9V^4 + 11.88V^3 + 3.2604V^2 - 0.4356V - 1.9879} - 0.09 \end{bmatrix}$$

with corresponding eigenvectors

$$v_{1,2} \approx \begin{bmatrix} 0.11 + 1.98V - 3V^2 + \sqrt{9V^4 + 11.88V^3 + 3.2604V^2 - 0.4356V - 1.9879} & 1 \\ 0.11 + 1.98V - 3V^2 - \sqrt{9V^4 + 11.88V^3 + 3.2604V^2 - 0.4356V - 1.9879} & 1 \end{bmatrix}$$

We plot the eigevalues to describe their dynamics in **Figure 1.2**.

Figure 1.2: Eigenvalues as a function of the steady state V^* for z. $\alpha = 0.01, \beta = 0.5, c = 0.1, z \in [0, 5]$

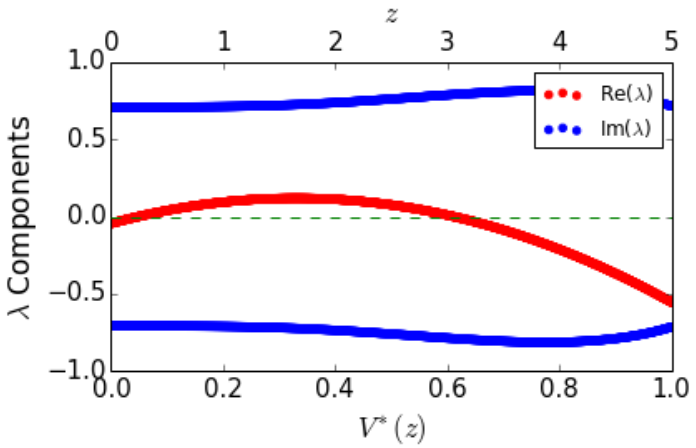

Note that the vertical axis of the above plot corresponds to the value of the eigenvalue, while the lower horizontal axis denotes the value of the steady state V^* for $z \in [0, 5]$ while the upper horizontal axis corresponds to the z value itself.

There is an observable bifurcation when the real component of the eigenvalue passes from negative to positive where $V^*(z) \approx 0$, and when the real component of λ passes from positive to negative near $V^*(z) \approx 0.6$. In **Figure 1.3** we confirm these values with a low resolution bifurcation (a) and subsequently confirm this with a tigher view of the left bifurcation point (b).

This is an example of a Hopf bifurcation at both of these instances. There is initially a fixed point which is stable, corresponding to no oscillation as well as a pair of complex conjugate eigenvalues. As z increases and reaches the first bifurcation, the fixed point loses stability and the stable limit cycle forms until z reaches the second bifurcation point and the limit cycle collapses back to the single stable fixed point as the real component

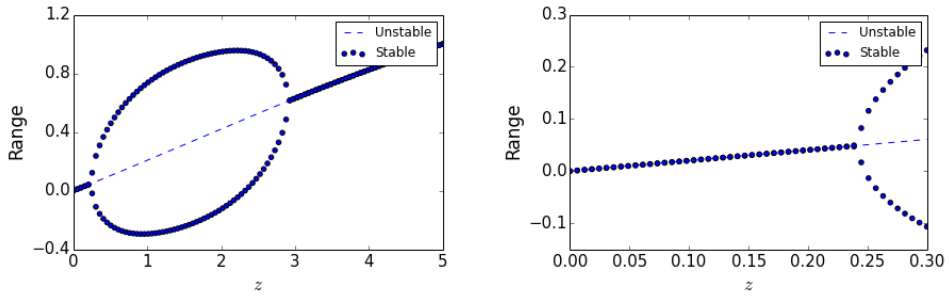

(a) Low resolution bifurcation diagram of the system. Stable limit of V plotted on the vertical axis while z is depicted on the horizontal. $\alpha = 0.01, \beta = 0.5, c = 0.1, z \in [0, 5]$. Steady state determined after 10,000 time steps.

(b) High resolution bifurcation diagram of the system. Stable limit of V plotted on the vertical axis while z is depicted on the horizontal. $\alpha = 0.01, \beta = 0.5, c = 0.1, z \in [0, 5]$ Steady state determined after 10,000 time steps.

Figure 1.3: Bifurcation diagrams for FN model.

of the eigenvalue once again becomes negative. We can visualize this stable limit cycle by plotting the phase plane of the system with a stable value of $z = 0.5$ in **Figure 1.4**.

Figure 1.4: Phase plane of the FN system. $\alpha = 0.01, \beta = 0.5, c = 0.1, z = 0.5$

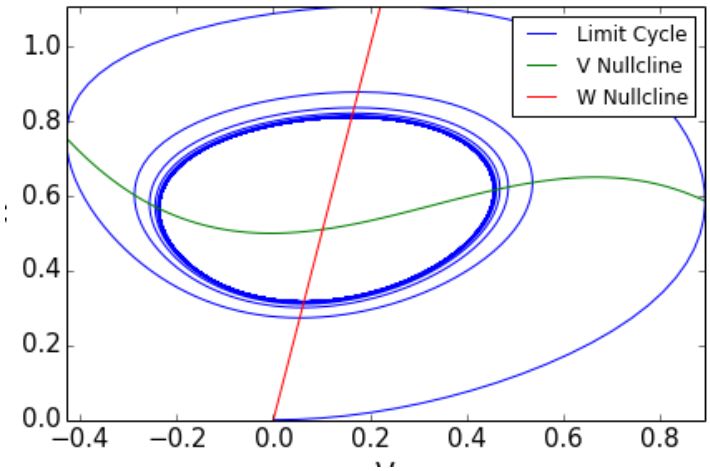

This clearly displays the system oscilating for a value of z.

1.5 Coupled Oscillators

The previously described model is useful for observing the dynamics of a single cardiac neuron, however occasionally researchers wish to incorporate several connected neuros in the same system.

Here we couple neurons, first two, then n, in a modified synfire chain. In this network, current passes through gap junctions and can only travel in one direction. Current flows from the first neuron (N_1) to the second neuron N_2 and sequentially through neurons N_i to N_n. When the current reaches the final neuron N_n, it is returned to the original neuron N_1. More formally, for a network of n oscillators Ω with members N_i; $i \in \mathbb{N}$ and $1 \leq i < j \leq n$ and $j \equiv i + 1$, N_i projects onto N_j and N_n projects onto N_1.

Conceptually, the model can be thought of as a circular path, though in reality this is a specific kind of boundary condition and has no physical interpretation.

From here on, we present only V and omit W from our analysis, as it is not advantageous to track both quantities. In order to couple neurons, we propose the following model to couple neurons N_A and N_B:

We connect oscillators with a gap junctional current $I_g = H(0.3 - V_x)G_g$ where $H(\cdot)$ is the heavyside function. For a population of n oscillators Ω, with members $N_i; i \in \mathbb{N}; 1 \leq i \leq n$. If $x; x \subset \Omega$ projects onto N_i then the gap junctional current to N_i is $\sum_x G_{x,i} H(0.3 - V_x)$

In the case of 2 oscillators (A and B)

$$\begin{aligned}
\frac{dV_A}{dt} &= V(\alpha + V_A)(1 - V_A) - W_A + G_g H(0.3 - V_B) + z_A \\
\frac{dV_B}{dt} &= V(\alpha + V_B)(1 - V_B) - W_B + G_g H(0.3 - V_A) + z_B \\
\frac{dW_A}{dt} &= \beta V_A - cW_A \\
\frac{dW_B}{dt} &= \beta V_B - cW_B
\end{aligned}$$

The purpose of heavyside thresholding is to implicitly create a spatial time dependence in the system. When an action potential reaches a neuron, a time delay occurs between spike incidence and propagation to the next member of the chain. By forcing propagation to occur only after the signaling member has spiked, implicitly creates a time dependence in intraneuron signal propagation.

Using the above model, we construct a system with two coupled neurons and graph their time series on the interval $t \in [0, 200]$ in **Figure 1.5**.

Observe that both neurons are out of phase by a constant amount.

Figure 1.5: Two coupled neurons. $\alpha = 0.01, \beta = 0.5, c = 0.1, z = 0.5$

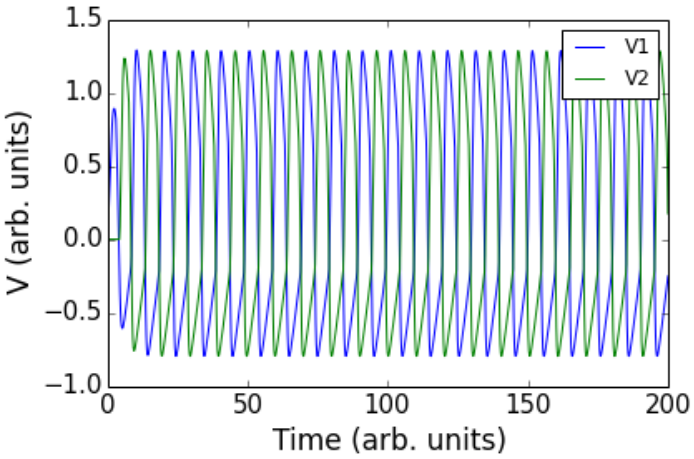

We further extend the model to couple n neurons in **Figure 1.6**.

Figure 1.6: $n = 5$ coupled neurons. $\alpha = 0.01, \beta = 0.5, c = 0.1, z = 0.5$

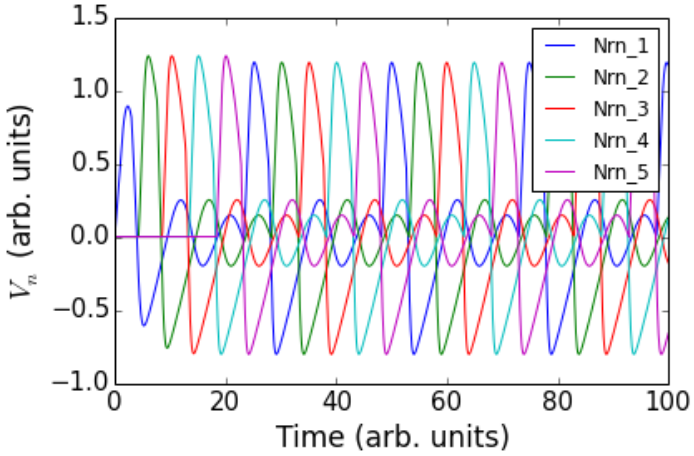

Note that the above has used paramters such that the stable limit cycle is sustained. We can use this extension to the FN model in order to answer biologically relevant questions about myocardial necrosis in the following section.

Additionally, we describe the frequency change as a function of the number of neurons in the system. As frequency (f) is defined by $\frac{1}{T}$, with increasing number of neurons, frequency decreases. At the extreme, as $\lim_{n\to\infty} f \to 0$.

Figure 1.7: System frequency as a function of neuron count. $\alpha = 0.01, \beta = 0.5, c = 0.1, z = 0.5$

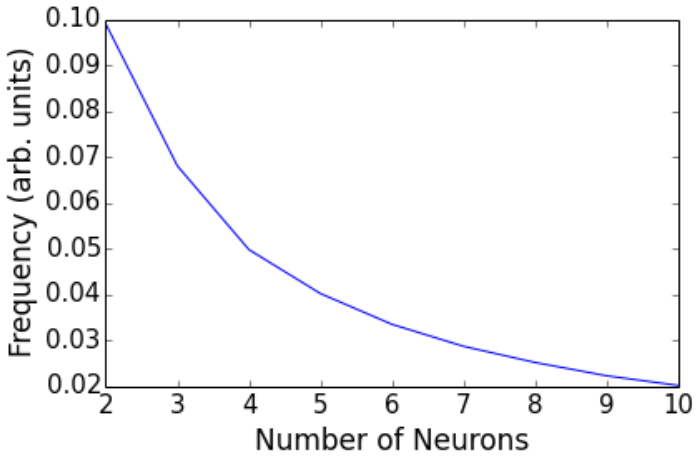

Note that the coupled system behaves as expected in **Figure 1.7**.

Chapter 2

Modelling Myocardial Necrosis

2.1 Translational Perspective

The heart serves a vital role in many organisms. The timely and regular delivery of oxygenated blood is essential to survival, and thus any decrease from optimum efficiency is of consequence. Investigations into potential mechanistic explainations and modeling of this degradation are highly interesting in the context of both accute and chronic cardiac disease.

In particular, myocardial necrosis can be caused by accute oxygen deprivation of myocardial tissues, commonly experienced during a heart attack. Other potential etiologies stem from depriving this tissue of the blood it requires; dangerous increase in physical stresses, coronary artery disease, and accute hemerage all have the potential to play into cardiac necrosis, perhaps in tandem.

In our investigation into the decreasing efficiency of a heart-like system, we will model several scenarios that may be of consequence to sufferers of cardiac necrosis. In particular, we study two cases. The first, static necrosis, closely resembles a short term or acute stress on myocardial tissue, be it a myocardial infarction or trauma. We will investigate how the distribution of necrosis affects the system as a whole through the FN model. Through a translation lens, this equates to the decrease in efficiency as a consequence of various kinds of trauma. The second case will be a slowly increasing level of necrosis. This more closely resembles coronary artery disease, which has the potential to starve the tissues of oxygen for many years, slowly leading to health deficits in older age.

Throughout the investigation, we refer to a cell's necrosis burden as analagous to a protein build up, though this simply refers to the degree of degredation for that specific cell.

Our proposed extension to the FN model plans to shed light on the geneisis, progression, and finally the consequences of myocardial necrosis.

2.2 Necrosis Propagation

As part of the normal cell cycle, programmed cell death (apoptosis) exists and it serves several purposes. In most cases, it is both irreversible and adaptive (beneficial) for the organism. However in some cases, apoptosis can occur accidentally in which case an irreversible destruction of the cell will occur. In our model, we assume that necrosis is a function of an underlying accumulation of pro-apoptotic proteins, potentially introduced as a byproduct of disease. As such, necrosis is a continuous state of each cell. For cell i of n, define pro-necrotic burden as ν_i, with total burden of the system equal to $\frac{1}{n}\sum_{i=1}^{n}\nu_i$. Note that $\nu_1, ..., \nu_n \in [0, 1]$ and is a monotonically increasing function with respect to time.

Starting with the Fitzhugh Nagumo model equivalent

$$\frac{dV}{dt} = V(\alpha + V)(1 - V) - W + z$$
$$\frac{dW}{dt} = \beta V - cW$$

2.3 Static Disease Burden

ν_i is defined as the proportion of channels damaged or lost in neuron N_i. We define this as the necrotic burden of neuron N_i. In this section we study the effects of an acute injury which leaves the patient with a sudden decrease in neuronal efficiency. We first develop a model for this situation, then use this model to investigate how the distribution of necrotic burden affects the system.

2.3.1 Disease Model

For the coupled oscillators representing cardiac myocytes, as the cells die through an apoptotic pathway, a fraction of their gap junctions $\nu \in [0, 1]$ will be destroyed, through cell decay.

In order to model disease, each myocyte will have a corresponding ν term, such that

$$\frac{dV_A}{dt} = V(\alpha + V_A)(1 - V_A) - W_A + (1 - \nu_A)G_g H(0.3 - V_B) + z_A$$
$$\frac{dV_B}{dt} = V(\alpha + V_B)(1 - V_B) - W_B + (1 - \nu_B)G_g H(0.3 - V_A) + z_B$$

With increasing ν, the cell becomes less responsive to its coupled partners.

We present the above model for both 2 (as a test case) and n coupled neurons with static necrosis term ν_i.

Figure 2.1: Static disease model in two neurons. $\alpha = 0.01, \beta = 0.5, c = 0.1, z = 0.5, \nu_1 = 0, \nu_2 = 0.5$

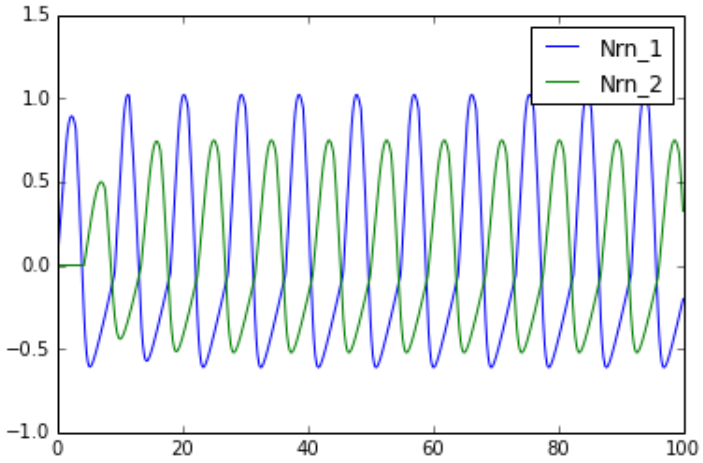

We use this model to answer biologically relevant questions.

2.3.2 Dispersion of Necrosis

We initially investigate how the distance between disease burdens may affect the cellular system.

Lemma: $\nu_i = 1$ is a trivial solution which will destroy the system every time, so from this point onwards it is excluded from all analyses.

Proof: Let Ω be a population of n neurons called $N_1, N_2, ..., N_{n-1}, N_n$. For any $1 \leq i \leq n$, if $\nu_i = 1$, $1 - \nu_i = 0$, and accordingly $(1 - \nu_i)G_g H(0.3 - V_{i+1}) + z_i = 0$ because $z_i = 0$ for any time above the initial impulse. Thus,

Figure 2.2: Static disease model in $n = 5$ neurons. $\alpha = 0.01, \beta = 0.5, c = 0.1, z = 0.5, \nu_1 = 0.1, \nu_2 = 0.1, \nu_3 = 0.1, \nu_4 = 0.1, \nu_5 = 0.1$

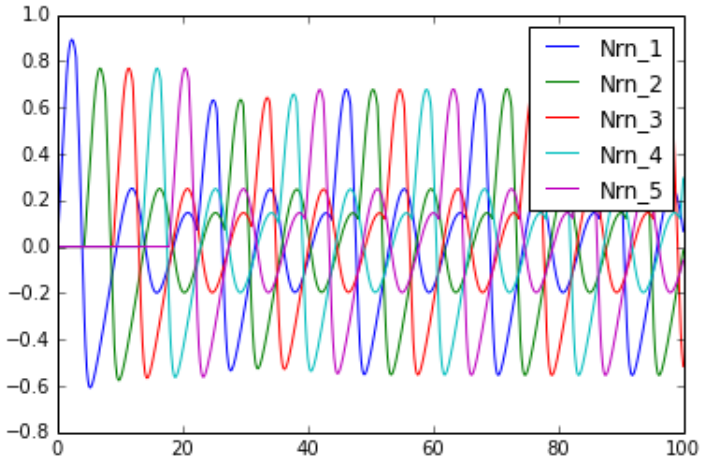

$I_m = (1 - \nu_i)G_g H(0.3 - V_{i+1}) + z_i = 0$ or the effective membrane current which is acting on the system is 0 for any $\nu_i = 1$. Following this logic, if $I_m = 0$ for any neuron i, N_i will have a negative real component to its eigenvalue λ, and thus will have only one steady fixed point solution and not enter a stable limit cycle. Because N_i will be fixed, N_{i+1} will become fixed, and the effect will propegate throughout the system Ω. In this way, $\nu_i = 1$ for any $1 \leq i \leq n$ will be a trivial solution to the system.

We hypothesize that the distance between disease burdens should not play a role in how effective they are in diminishing the system's efficacy.

To lend evidence to our hypothesis, we construct two systems A and B, labelled accordingly. In system A, we impose a disease burden on dispersed cells. We damage N_1 and N_3, leaving all others unaffected ($\nu_i = 0$ for all others). We define $\nu_1 = 0.5$ and $\nu_3 = 0.5$. We plot the solution to the system and observe that, though there are ramifications and the system appears more spastic, it is systained. In system B, we impose sequential burdens such that $\nu_1 = 0.5$ and $\nu_2 = 0.5$, leaving all others unburdened ($\nu_i = 0$). In this case in **Figure 2.3**, we observe a rapid collapse of the system.

We interpret these results at the end of this section.

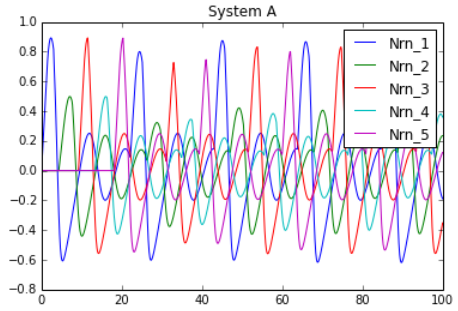

(a) Dispersed necrotic burden in a static disease model. $\nu_{1,3} = 0.5, \nu_{2,4,5} = 0, \alpha = 0.01, \beta = 0.5, c = 0.1$

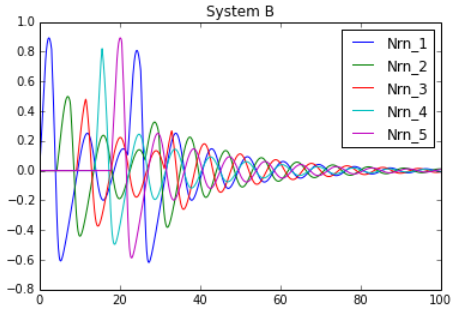

(b) Sequential necrotic burden in a static disease model. $\nu_{1,2} = 0.5, \nu_{3,4,5} = 0, \alpha = 0.01, \beta = 0.5, c = 0.1$

Figure 2.3: Examining the effects of dispersion on system performance in a static model.

2.3.3 Density of Necrosis

We proceed to investigate whether few large burdens or multiple smaller burdens may affect the system more. We construct two systems A and B such that $\sum_{i=1}^{n} \nu_{Ai} = \sum_{i=1}^{n} \nu_{Bi}$ but choose to minimize the burden in each cell for system A, while we concentrate it in a single neuron for system B. We chose to assign $\nu_{1,2,3,4,5} = 0.15$ for system A and $\nu_3 = 0.75$ for system B. System A appears to sustain itself while system B rapidly collapses as in **Figure 2.4**. We interpret these results in the following section.

2.3.4 Discussion

From the analsysis above, we lend support to the ideas that the worst (most destructive) necrosis in a system would be a clustered, concentrated increase in necrosis. In practice, this means that a sudden traumatic incident such as an acute occlusion of a cardiac blood vessel would have a must more direct impact than a chronic condition slowly necrotizing tissue.

More sophisticated mehthods would be required to ascertain the bounds on these conditions due to the high dimensionality of the system. At this point of the analysis we can only lend evidence to the above ascertation. We continue this analysis with the development of a dynamic evolution of the ν necrosis burden.

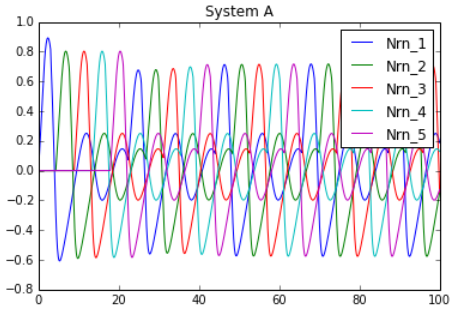

(a) Minimal necrotic burden in a single neuron for a static disease model. $\nu_{1,2,3,4,5} = 0.15, \alpha = 0.01, \beta = 0.5, c = 0.1$

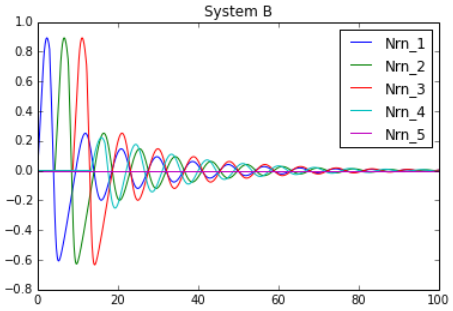

(b) Maximal necrotic burden in a single neuron for a static disease model. $\nu_3 = 0.75, \nu_{1,2,4,5} = 0, \alpha = 0.01, \beta = 0.5, c = 0.1$

Figure 2.4: Examining the effects of density on system performance in a static model.

2.4 Dynamic Disease Burden

In order to extend this model to model cardiac necrosis, we use the previously described coupling and staic model, adding ν_i as an ordinary differential equation describing the dampening on neuron i (N_i). In the present simplication, ν_i will depend only on time. Define ν_{0i} as the *a priori* necrotic burden of N_i.

2.4.1 Disease Model

We wish to construct a model of ν_i evolution where, eventually, the disease will destroy the cell. Thus, we wish to have 1 (complete dampening) as a stable steady state. Additionally, we require that any concentration of ν_{0i} will eventually lead to cell death. We chose the following model and plot it in **Figure 2.5**:

$$\frac{d\nu_i}{dt} = \dot{\nu} = \nu_i(1 - \nu_i)$$

Giving a distribution of the rate of change corresponding to the following:

Note that in this model, $\nu_i = 0$ is an unstable steady state while $\nu = 1$ is a stable steady state. This is desirable for the model, and intuitivly means that any amount of ν_i will eventually go to 1 and stop the system.

We demonstrate the above model in a two neuron system in **Figure 2.6**.

Figure 2.5: Differential Equation describing the evolution of ν_i with respect to time.

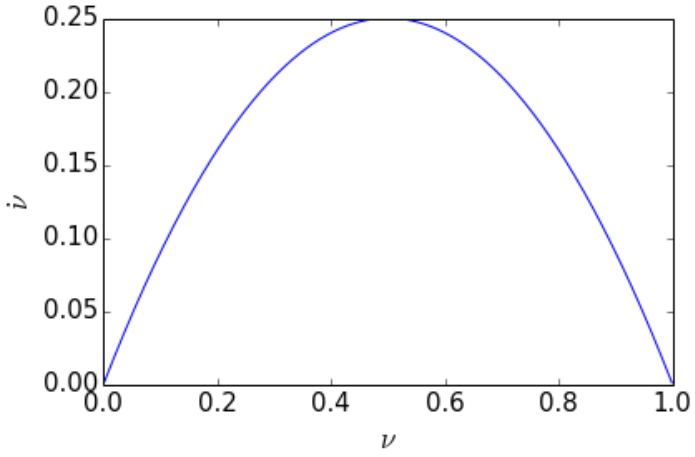

Figure 2.6: Dynamic disease model in two neurons. $\alpha = 0.01, \beta = 0.5, c = 0.1, z = 0.5, \nu_1 = 0.01, \nu_2 = 0$

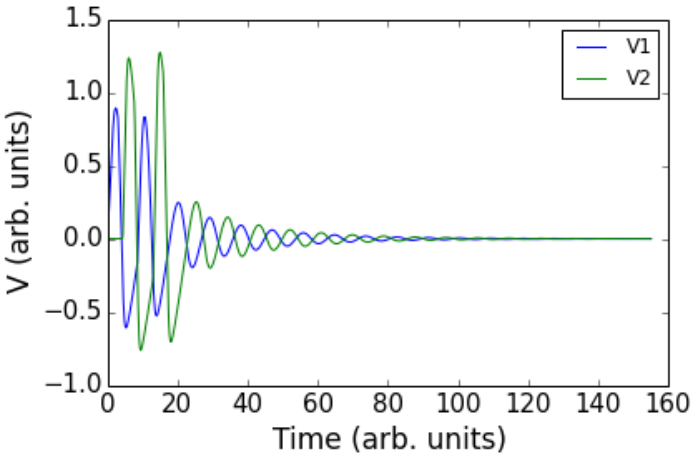

And also in a system with $n = 5$ neurons in **Figure 2.7**.

2.4.2 Dispersion of Necrosis

We repeat the above analysis for the dynamic system. First we create a system A with initial dispursed necrosis such that $\nu_{1,3} = 0.1$ and $\nu_{2,4,5} = 0$.

Figure 2.7: Dynamic disease model in five neurons. $\alpha = 0.01, \beta = 0.5, c = 0.1, z = 0.5, \nu_1 = 0.01, \nu_2 = 0, \nu_3 = 0, \nu_4 = 0, \nu_5 = 0$

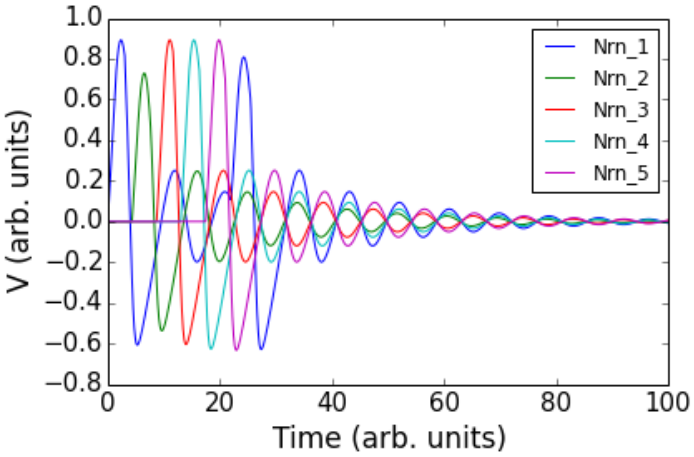

We additionally construct a second system B such that the initial necrosis is clustered, $\nu_{1,2} = 0.1$ and $\nu_{3,4,5} = 0$. We plot the solution to the system in **Figure 2.8** and observe no radical difference between the two systems.

We discuss implications of the above in the next section.

2.4.3 Density of Necrosis

Additionally, we examine the effect of necrosis density on system performance and plot in **Figure 2.9**. We create a system A where all of the initial necrosis is concentrated in a single neuron such that $\nu_3 = 0.5$ and $\nu_{1,2,4,5} - 0$. We compare this to system B where we give each neuron a smaller level of disease burden such that $\sum_{i=1}^{n} \nu_{Ai} = \sum_{i=1}^{n} \nu_{Bi}$. In system B we define $\nu_{1,2,3,4,5} = 0.1$.

We interpret the above in the following section.

2.4.4 Discussion

By using our model, we demonstrate that the distribution of initial necrosis does not affect, or at least does not meaningfully effect, the degredation of the system. Additionally we found that a system with lower initial concentrations in many neurons more rapidly destroys the system than a higher initial concentration in a single neuron.

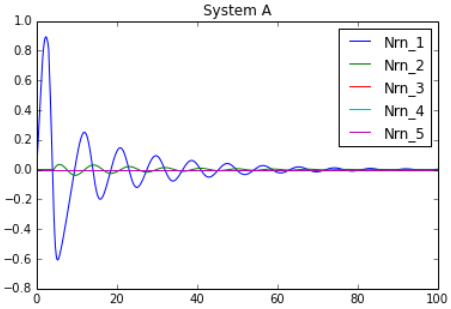

(a) Dispersed necrotic burden in a dynamic disease model. $\nu_{1,3} = 0.1, \nu_{2,4,5} = 0, \alpha = 0.01, \beta = 0.5, c = 0.1$

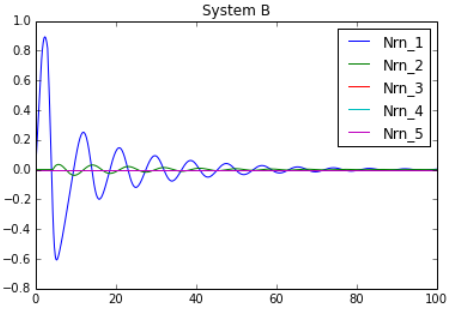

(b) Sequential necrotic burden in a dynamic disease model. $\nu_{1,2} = 0.1, \nu_{3,4,5} = 0, \alpha = 0.01, \beta = 0.5, c = 0.1$

Figure 2.8: Examining the effects of dispersion on system performance in a dynamic model.

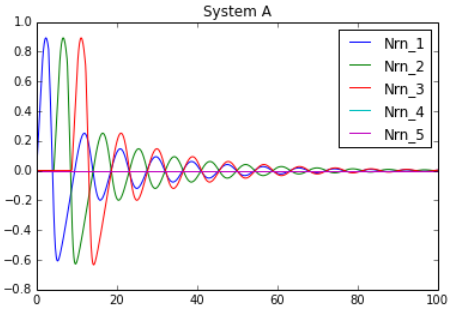

(a) Minimal necrotic burden per neuron in a dynamic disease model. $\nu_{1,2,3,4,5} = 0.1, \alpha = 0.01, \beta = 0.5, c = 0.1$

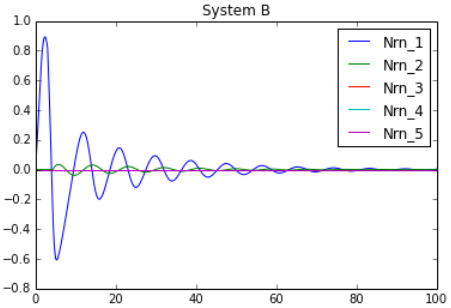

(b) Sequential necrotic burden in a dynamic disease model. $\nu_3 = 0.5, \nu_{1,2,4,5} = 0, \alpha = 0.01, \beta = 0.5, c = 0.1$

Figure 2.9: Examining the effects of density on system performance in a dynamic model.

Intuitively this tells us that a more dispersed illness which is evolving will have a more devastating effect than a locally contained one.

2.5 Conclusion

In summary, we present an examination of the Fitzhugh Nagumo model for relaxation oscillators, a simplication of the original Hodgkin-Huxley. We analyze the stability of this model and provide insight into its dynamics. In addition to the base model, we develop three extensions. Firstly, we develop a method for the coupling of multiple neurons, allowing us to simulate a modified synfire chain. Using this coupling method, we introduce a new term ν to represent the proportion of destroyed ion channels as a result of myocardial necrosis. We introduce this term into our coupling extension first as a parameter, and second as differential equation tracking disease progression. We use these extensions to make statements related to disease prognoses and the differences amung various situations.

The modelling of biological systems represents a crucial cog in the machine developing solutions to medicinal problems. With our extension, we take a further step towards undstanding the etiology of various diseases sharing a genesis involving cardio-hypoxic events such as strokes and acute trauma. Our model has wide implications from myocardial infarction to drug delivery to carcinogenic pathways. More work must be done in this area to correctly model these disease *in silico*. Only by understanding the pathways and processes involved in disease can we hope to combat it, and eventually, to beat it.

Chapter 3

Additional Material

3.1 Web App

3.1.1 Description of Model

In addition to the previous analysis, we present an interactive model to observe the effects of various combinations of parameters. The application, at present, only performs analysis for the static case of the model.

The application is written in the programming language R 3.2.2 and hosted on shinyapps in **Figure 3.1**. The app can also be built locally.

The application uses the forward Euler method for solving differential equations, and the user is invited to see the effects of changing any parameter on the system's behavior. Please find the web application running at

https://ccole.shinyapps.io/fn_ex

Figure 3.1: Interactive visualization of two coupled neurons following the FN model with extension.

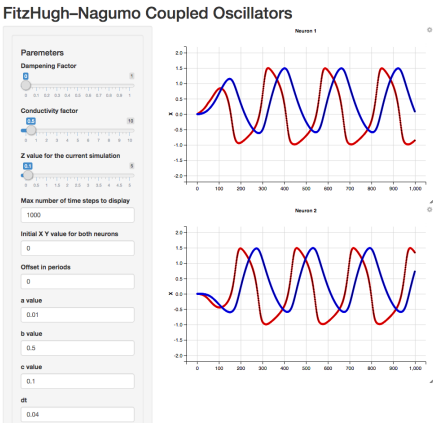

3.1.2 Building locally

To build the application locally, clone the git repo to your system and change your directory to the shiny repository. Start R.

```
$ git clone https://github.com/aaronshifman/modeling_final.git
$ cd modeling_final/shiny
$ R
```

ite

The web app has several dependencies. The following packages must be installed:

1. ggvis
2. shiny
3. deSolve

Once installed, type RunApp() into the R console. The application will display in a viewer.

3.2 Additional Visualizations & Supporting Information

Dynamic Visualizations

Please visit the following webpage to view the online-only supplemental material

http://nbviewer.ipython.org/github/aaronshifman/modeling_final/blob/master/ipynb/Supplemental_Material.ipynb

The website containes two visualizations with associated code:
Figure S1: Sweep of phase plane for $z \in [0, 5]$
Figure S2: Coupling animation for $\nu \in [0, 1]$
Please note that all code and associated analyses are hosted in an open source Github repository, found here:

https://github.com/aaronshifman/modeling_final

Chapter 4

References

1. Abbott, L. . Lapicques introduction of the integrate-and-fire model neuron 1907. Brain Res. Bull. 50, 303304 1999.

2. Hodgkin, A. L., Huxley, A. F. A quantitative description of membrane current and its application to conduction and excitation in nerve. J. Physiol. 117, 50044 1952.

3. Haefner, J. W. Models of Systems. Modeling Biological Systems: Principles and Applications *Springer*, 2005. doi:10.1007/0-387-25012-3_1

4. 1. Izhikevich, E. M. Dynamical Systems in Neuroscience. MIT Press (2006).